



Al_2S_3 , $\text{Al}_2\text{S}_3/\text{NiS}$ Nanomaterials Synthesis, Characterization and Photocatalytic Activity under Sunlight

K. P. Samskruthi and Sannaiah Ananda*

Department of Studies in Chemistry, University of Mysore, Mysuru, **INDIA**

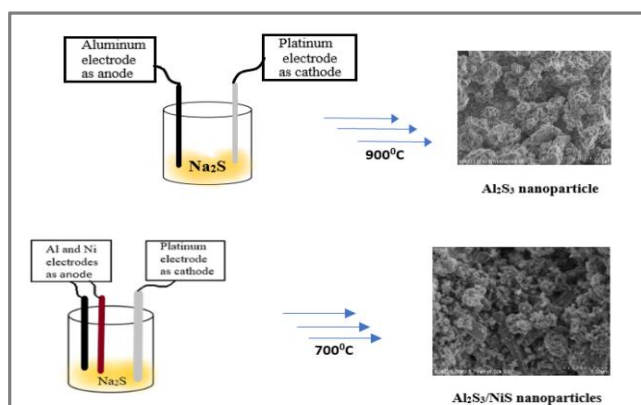
Email: snananda@yahoo.com

Accepted on 28th August, 2021

ABSTRACT

Al_2S_3 , $\text{Al}_2\text{S}_3/\text{NiS}$ nanomaterials have been synthesized by electrochemical method which is simple and inexpensive method. The synthesized Al_2S_3 , $\text{Al}_2\text{S}_3/\text{NiS}$ nanomaterials were used as a photocatalyst for the degradation of Methylene blue dye under sunlight. Nanomaterials synthesized by electrochemical method were characterized by various techniques such as SEM-EDAX, UV-Visible spectroscopy, FT-IR spectrum and X-ray diffraction studies. The UV-Vis spectroscopy study revealed that the band gap energy of $\text{Al}_2\text{S}_3/\text{NiS}$ nanocomposite to be 2.77 eV by Tauc plot. The presence of Aluminium, Nickel and Sulphur in the nanomaterial is confirmed from the EDAX spectrum. A FT-IR spectrum reveals the presence of characteristic bands corresponding to aluminium and nickel sulfides. The structure of $\text{Al}_2\text{S}_3/\text{NiS}$ nanocomposite was found to be hexagonal structure and crystal size was found to be 32 nm which was confirmed from XRD data.

Graphical Abstract



Electrochemical synthesis of Al_2S_3 and $\text{Al}_2\text{S}_3/\text{NiS}$ nanomaterials

Keywords: Al_2S_3 , $\text{Al}_2\text{S}_3/\text{NiS}$, Nanomaterial, Photodegradation.

INTRODUCTION

Nanomaterials are being pursued extensively because of their crystal structures, optical, magnetic, electrical and catalytic properties, structure, size and shape dependent [1-4]. It is known that metal sulfides exhibited interesting electronic properties and achieved several technological applications [5]. Environmental pollution associated with organic pollutants provide the impetus for sustained fundamental and applied research in the area of environmental remediation. Semiconductor acts as photocatalyst, which offers the potential for complete elimination of toxic chemicals through its efficiency and potentially broad applicability [6]. Effluents from textile, paper, and agro-industries are contaminated with chemicals such as dyes, phenols, and pesticides [7]. Dye-related industries such as textile, release various organic pollutants to the atmosphere. If these pollutants are discharged into the environment without any treatment, it will cause considerable toxicity to the various forms of lives. In order to get rid of this potential danger of these organic dyes, many technologies have been developed to treat these pollutants. Photocatalysis is an alternative route for water purification [8]. Aluminum sulfide, Al_2S_3 , is a colorless solid with a variety of crystalline structures [9]. Transition metal (TM) sulfides exhibit interesting optical, electronic, thermoelectric and photoelectric properties [10, 11]. Nickel sulfide (NiS) an important member of this large family of transition metal sulfides with a band gap 4.8eV and 2.8eV [12]. Different methods have been used in the literature for the synthesis of nanomaterials. Besides traditional methods of their production such as solvothermally [13], solid state reactions [14], solution synthesis [15] and electrochemical methods have widely employed in the synthesis of various nanoparticles [16]. Electrochemical method is preferred method, which is simple, reliable and inexpensive method [17, 18].

In this article, synthesis of Al_2S_3 and $\text{Al}_2\text{S}_3/\text{NiS}$ nanomaterials and their application in the photodegradation of Methylene blue dye [MB] was reported.

MATERIALS AND METHODS

All chemicals used in this work were of accepted grades of purity. Al and Ni metal wires, Sodium Bicarbonate purchased from Alfa-Aesar and Indigo carmine dye from Merck. All solutions were prepared in double distilled water. Optical absorption spectra were recorded at room temperature, on JASCO- UV-Vis spectrophotometer. The crystallographic interpretations were performed by X-ray diffractometer (Rigaku miniflex II desktop X-ray diffractometer), using Cu/α wavelength ($\lambda=1.54\text{\AA}$). The morphological feature of the semiconductor was observed by scanning electron microscopy (Zeiss Evo LS15). The elemental analysis of the nanoparticles is confirmed, from Energy dispersive X-ray analysis (EDAX), recorded on HITACHI S-3400N JAPAN.

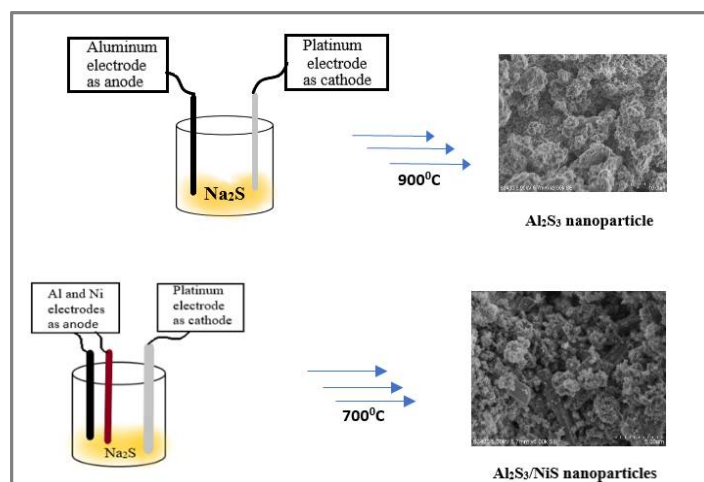
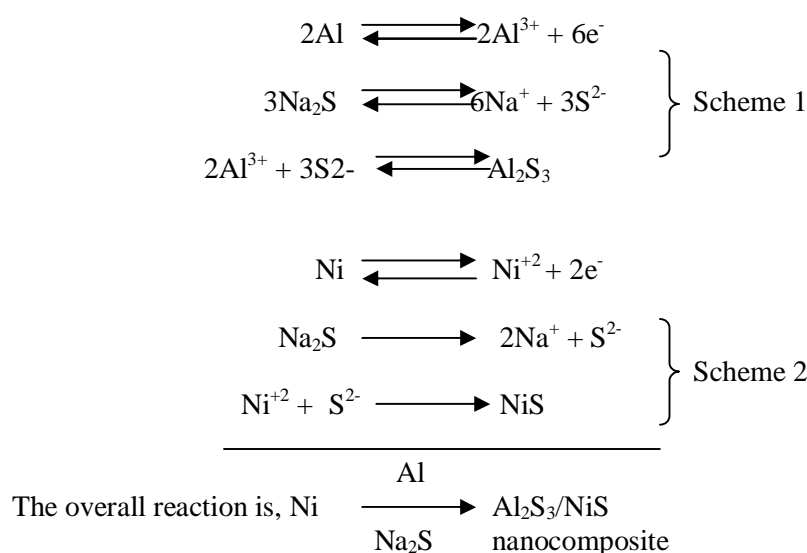


Figure 1. Electrochemical synthesis of Al_2S_3 and $\text{Al}_2\text{S}_3/\text{NiS}$ nanomaterials.

Electrochemical synthesis of Al_2S_3 and $\text{Al}_2\text{S}_3/\text{NiS}$ nanomaterials: Al_2S_3 and $\text{Al}_2\text{S}_3/\text{NiS}$ nanomaterials were synthesized by electrochemical method. For the synthesis of Al_2S_3 nanomaterial Al metal wire is used as anode and platinum electrode is used as cathode. The experiment was run for 3h (20mA, 10V) (Figure 1). The anodic dissolution of Al to give Al(III) ions which are electrochemically reacted with aqueous Na_2S (0.2M) to form Al(III) sulphides as shown in scheme 1.

Likewise, for the synthesis of $\text{Al}_2\text{S}_3/\text{NiS}$ nanocomposite, Ni and Al metal wires are used as anodes and platinum electrode as cathode. The experiment was run for 3h with continuous stirring (20mA, 10V). The anodic dissolution of Al and Ni to give Al(III) and Ni(II) ions which are electrochemically reacted with aqueous Na_2S (0.2M) to form nanocomposite of Al(III) and Ni(II) sulphides in scheme 2. The solid obtained in both the scheme was washed with double distilled water till complete removal of unreacted Na_2S . Then the solid is centrifuged and calcined for 2 h from 700°C to 900°C for dehydration and for the removal of sulphur and other impurities to get Al_2S_3 and $\text{Al}_2\text{S}_3/\text{NiS}$ [16, 23, 31].

The rate of electrochemical reaction is not same for all the metals, as the redox potential of Al and Ni is different. The rate of dissolution for Al (-1.706V) is faster than Ni (-0.23V) so that higher portion of Al(III) or Al_2S_3 is formed than Ni(II) or NiS in $\text{Al}_2\text{S}_3/\text{NiS}$ nanocomposite. The electrochemical reaction takes place according to the following mechanism.



Scheme 1 and 2. Reaction for the formation of Al_2S_3 and $\text{Al}_2\text{S}_3/\text{NiS}$ nanomaterials.

Determination of Photocatalytic activities: Methylene Blue (MB) solution was prepared by dissolving g 100 mL^{-1} in distilled water. This solution was then used as a test contaminant for investigating photocatalytic activities of the synthesised Al_2S_3 and $\text{Al}_2\text{S}_3/\text{NiS}$ nanomaterials. The evaluation was carried out sunlight in order to investigate the efficiency of Al_2S_3 and $\text{Al}_2\text{S}_3/\text{NiS}$ nanomaterials. Chemical oxygen demand (COD) was estimated before and after treatment using dichromate oxidation method [22, 32]. The increase in percent transmission and decrease in COD (m/L^{-1}) of the dye solution with color removal was observed to be more in Al_2S_3 compared to $\text{Al}_2\text{S}_3/\text{NiS}$ nanocomposite. The COD has obtained by using the equation (1).

$$\text{COD} = \frac{(\text{Blank} - \text{Sample}) \times N_{\text{FAS}} \times 8000}{V_{\text{sample}}} \quad \dots (1)$$

RESULTS AND DISCUSSION

Scanning Electron Microscope (SEM): The surface morphology of Al_2S_3 and $\text{Al}_2\text{S}_3/\text{NiS}$ nanomaterials were investigated by SEM. The SEM morphology (Figure 2) revealed that sample consist of aggregation of particles with spherical and hexagonalcrystal like structure. The EDAX confirms the presence of Al, Ni and S in the synthesized Al_2S_3 and $\text{Al}_2\text{S}_3/\text{NiS}$ nanomaterials (Figure 3).

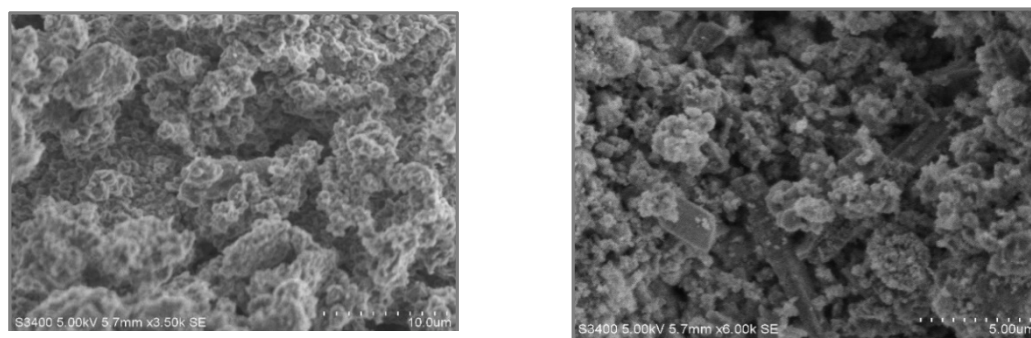


Figure 2. SEM images of Al_2S_3 and $\text{Al}_2\text{S}_3/\text{NiS}$ nanomaterials.

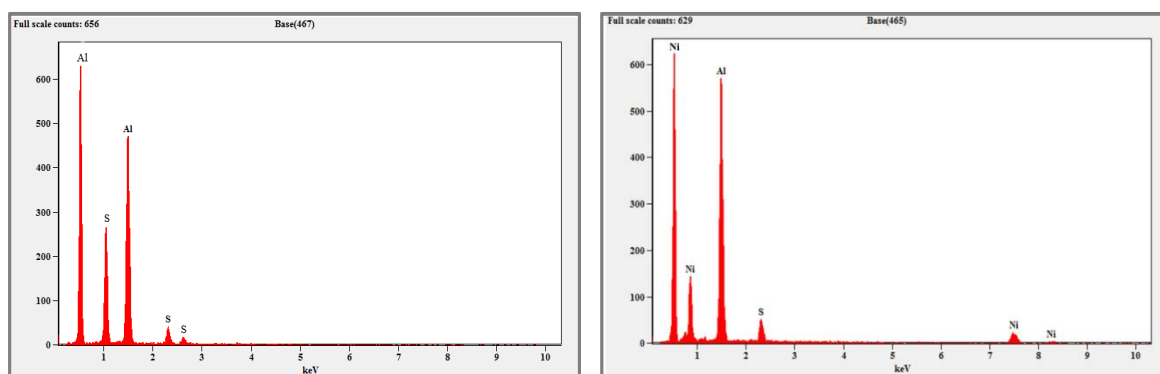


Figure 3. EDAX of Al_2S_3 and $\text{Al}_2\text{S}_3/\text{NiS}$ nanomaterials.

X-ray diffraction: X-ray diffraction (XRD) peaks of $\text{Al}_2\text{S}_3/\text{NiS}$ matched with the hexagonal structure. $\text{Al}_2\text{S}_3/\text{NiS}$ powder showed high intensity diffraction peaks (101), (102), (110), (006), (113), (116), (300), (119) at $2\theta = 16.7, 18.8, 27.8, 30.0, 31.4, 41.4, 49.2$ and 54.4 (JCPDS Card # 00-047-1313) (Figure 4) [21,22].

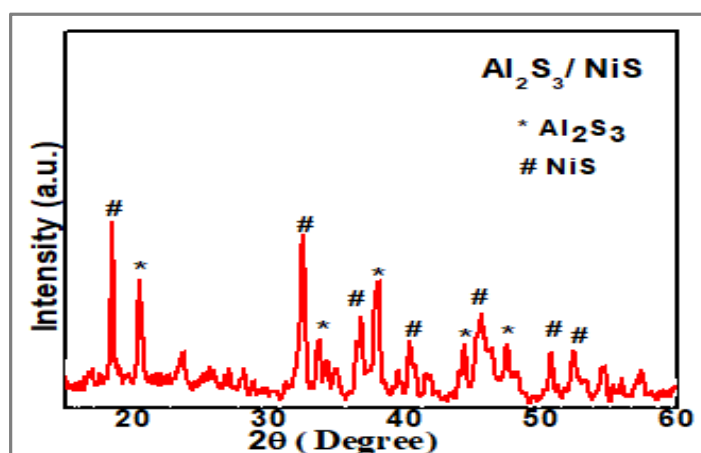


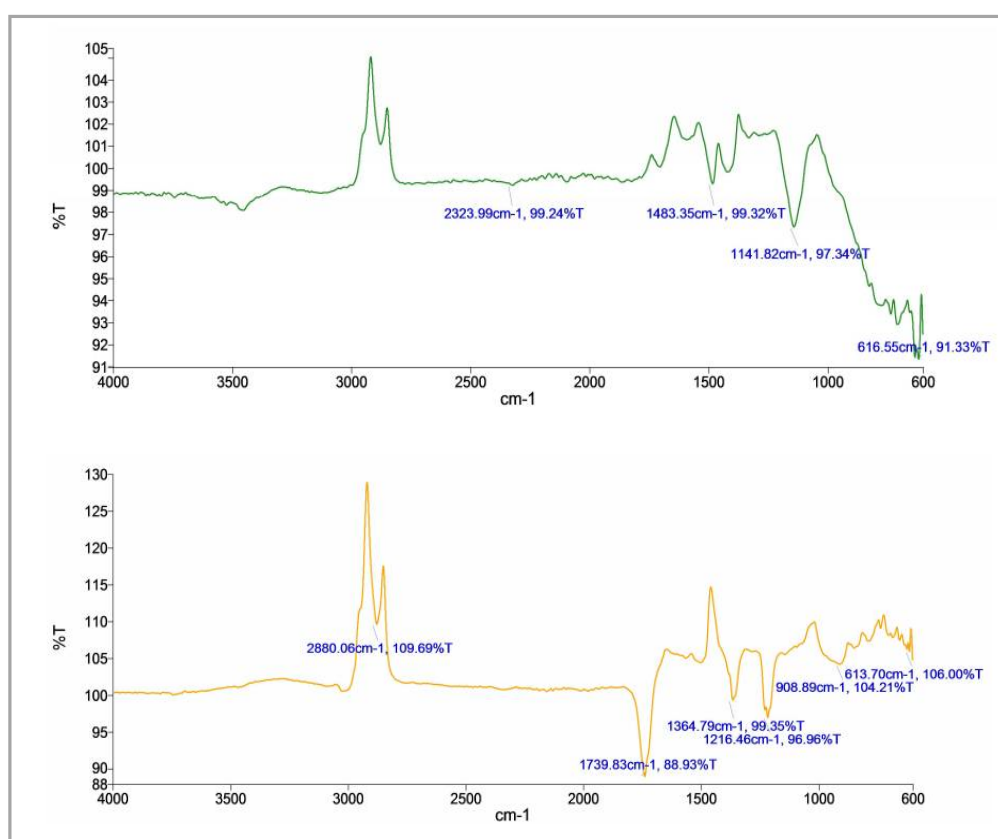
Figure 4. XRD patterns of $\text{Al}_2\text{S}_3/\text{NiS}$ nanocomposite.

The following Debye Sherrer formula was used to determine the average size of the $\text{Al}_2\text{S}_3/\text{NiS}$ nanocomposite and confirmed from the Williamson-Hall plot.

$$D = 0.9\lambda/\beta \cos\theta \dots(2)$$

Where, λ is X- ray wavelength, β is the full width at half maximum and θ is the Bragg angle [23]. The average grain size calculated from the above formula was found to be about 32 nm.

FT-IR Analysis: Fourier transform infrared (FTIR) analysis was performed to confirm the presence of functional groups on the surface of samples. Figure 5 represents the IR spectrum of the Al_2S_3 and $\text{Al}_2\text{S}_3/\text{NiS}$ nanomaterials. Peak at 1115 cm^{-1} is asymmetrical stretching assigned to sulphides [23], while bands at 394, 419, 442, 668 and 765 (symmetrical stretch) and 1060 cm^{-1} (asymmetrical stretch) are assigned to sulfides, which indicates the presence of nanosized NiS [24, 25].

**Figure 5.** FTIR spectrum of Al_2S_3 and $\text{Al}_2\text{S}_3/\text{NiS}$ nanomaterials.

UV-visible spectrum: UV-Visible spectrum of $\text{Al}_2\text{S}_3/\text{NiS}$ over the range of 200-400 nm showed that the synthesized nanoparticles are photoactive under visible light irradiation. The band gap of $\text{Al}_2\text{S}_3/\text{NiS}$ was calculated using Tauc plot (Figure 6). For a semiconductor sample, it is possible to determine the optical absorption near the band edge by the equation, $\alpha hv = A(hv - E_g)^{n/2}$ where α , h , v , E_g and A are absorption coefficients, plank's constant, radiation frequency, band gap and a constant respectively. The n value decides the characteristics of the transition in a semiconductor being 1 or 4 respectively, for a direct or an indirect semiconductor. In order to get an accurate value of the band gap of solids, it is necessary to construct a $(\alpha hv)^{1/2}$ versus hv also called Tauc plot [24]. From the optical absorption spectra it is clear that synthesized $\text{Al}_2\text{S}_3/\text{NiS}$ nanocomposite has showed the maximum intensity peak at 447 nm. The band gap of the samples Al_2S_3 and $\text{Al}_2\text{S}_3/\text{NiS}$ is calculated

using Tauc plot by plotting $(\alpha h\nu)^{1/2}$ v/s $h\nu$ and it is found to be 2.5eV and 2.77eV respectively. The band gap of NiS (3.75eV) and $\text{Al}_2\text{S}_3/\text{NiS}$ is higher than that of Al_2S_3 . This supports lower photocatalytic efficiency of $\text{Al}_2\text{S}_3/\text{NiS}$ nanocomposite compared to Al_2S_3 after the formation of $\text{Al}_2\text{S}_3/\text{NiS}$ nanocomposite [29, 30].

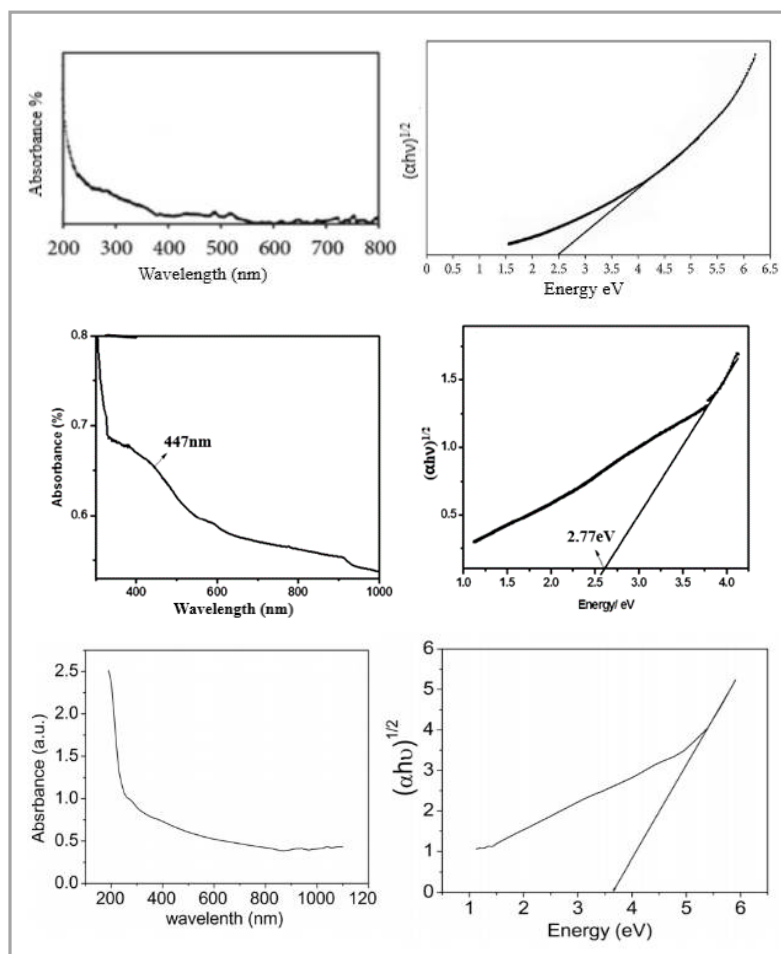
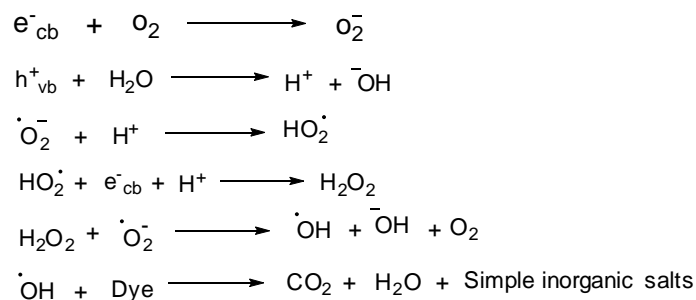


Figure 6. UV spectra of Al_2S_3 , $\text{Al}_2\text{S}_3/\text{NiS}$ and NiS nanomaterials.

Determination of photo catalytic activities: Photo degradation assisted by semiconductor depends on various parameters like nature and concentration of the organic substrates, concentration and type of semiconductor, light source and intensity, pH, temperature [18]. Photo degradation experiments were carried out using different concentration of Methylene blue dye as substrate and different amounts of Al_2S_3 and $\text{Al}_2\text{S}_3/\text{NiS}$ nanomaterials as a photocatalyst. A calculated quantity of the catalyst was added to the dye solution. Stirred in the dark to establish equilibrium between the dye and nanoparticle molecules and then illuminated under sunlight to induce the photochemical reaction. Aliquots were taken at an interval of 30min to determine the change of %T using Elico SL 171 (g%) was calculated as follows [20,33].

$$\text{Photodegradation efficiency} = \frac{\text{Initial COD} - \text{Final COD}}{\text{Initial COD}} \times 100 \quad \dots (3)$$

Effect of Catalyst Loading: The experiments were performed by taking different amount of catalyst varying from 1.0 mg to 4.0 mg in order to study the effect of catalyst loading. The study showed that increase in catalyst loading from 1.0 mg to 3.0 mg increased dye removal efficiency. Further increase in catalyst above 3.0 mg decreased the photoactivity of the catalyst, which is due to the aggregation of



Scheme 3. Mechanism for the photo degradation of dye.

nanoparticles at high concentration causing a decrease in the number of surface active sites and increase in the opacity and light scattering of Al_2S_3 and Al_2S_3/NiS nanomaterials at high concentration. This tends to decrease the passage of light through the sample. Further, the present study indicates, from economic point of view, the optimized photocatalyst loading is $3.0 \text{ mg } 20 \text{ mL}^{-1}$ (Figure 7 and 10, Table 1 and 2).

Table 1. Results of photodegradation of MB using Al_2S_3 nanomaterial

Variation	Amount of catalyst/dye	Rate constant $k \text{ s}^{-1} \cdot 10^{-5}$	Experimental Time (min)	COD values in mg mL^{-1}		Degradation Efficiency (%)
				Before degradation	After Degradation	
Amount of catalyst ($2 \times 10^{-5} \text{ M dye}$)	0.01g	5.75	210		121	86.8
	0.02g	6.91	180	914	98	89.2
	0.03g	8.82	150		75	91.7
	0.04g	5.37	210		118	87.1
Concentration of dye (0.02 g catalyst)	$1 \times 10^{-5} \text{ M}$	8.83	90	823	89	89.2
	$2 \times 10^{-5} \text{ M}$	6.91	180	914	103	88.6
	$3 \times 10^{-5} \text{ M}$	6.14	210	1123	182	83.8
	$4 \times 10^{-5} \text{ M}$	5.76	210	1256	221	82.4
pH ($2 \times 10^{-5} \text{ M dye}$, 0.02 g catalyst)	4	3.0	210	914	142	84.5
	6	2.3	210	914	168	81.6
	8	5.4	210	914	121	86.8
	10	3.0	210	914	141	84.6
Re-use of catalyst (0.02 g)	$2 \times 10^{-5} \text{ M}$	6.52	180	914	110	87.9

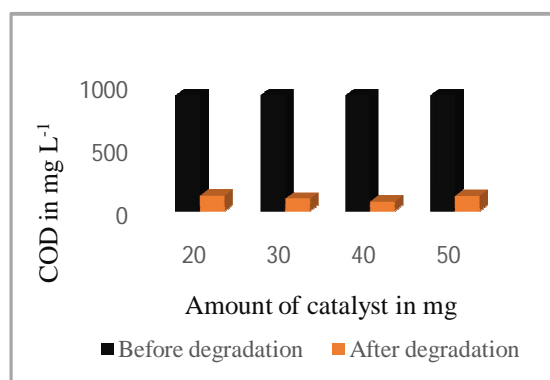
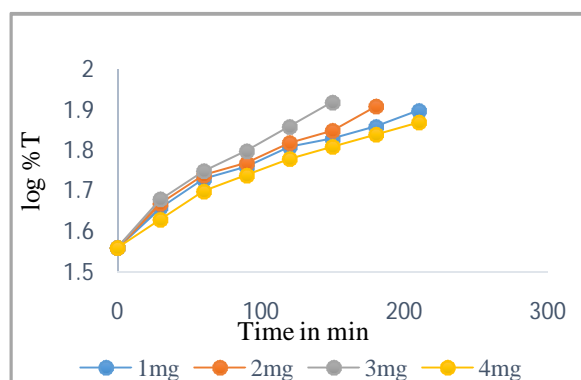


Figure 7. Plot of Log%T Vs Time for Different Amounts of catalyst (a) and Effect of COD upon degradation (b) using Al_2S_3 nanomaterial.

Effect of concentration of dye on degradation: The reaction was performed with different concentration of Methylene blue dye with constant weight of Al_2S_3 and $\text{Al}_2\text{S}_3/\text{NiS}$ catalyst. The change in concentration of the Methylene blue was recorded by change in colour using Spectrophotometer. A plot of $\log\%T$ (percent transmittance of light) versus time was linear and follows first order kinetics (Figure 8 and 11). The rate constant values are tabulated in table 1 and 2 and the reaction rate decreases with increase in concentration of MB. This is because with increase in the dye concentration, the solution becomes more intensely colour and the path length of the photons entering the solution is decreased thereby few photons reaches the catalyst surface. Hence the production of hydroxyl radicals is reduced. Therefore the photodegradation efficiency is reduced. The COD for MB solutions before and after degradation were measured and given in Table 1 and 2. To account for the mineralization of dye COD was determined at different stage. The formation of different radical species during photodegradation is given in scheme 3. The dye was found to have mineralized into H_2O , CO_2 and simpler inorganic salts [18, 19], after being irradiated for 3 and 1/2 h using Al_2S_3 and $\text{Al}_2\text{S}_3/\text{NiS}$ photocatalyst. $\text{Al}_2\text{S}_3/\text{NiS}$ catalyst shows no reaction at $3 \times 10^{-5}\text{M}$ and $4 \times 10^{-5}\text{M}$ concentration of dye.

Table 2. Results of Photodegradation of MB using $\text{Al}_2\text{S}_3/\text{NiS}$ nanomaterial

Variation	Amount of catalyst/ dye	Rate constant $k \text{ s}^{-1} 10^{-5}$	Experimental Time (min)	COD values in mg mL^{-1}		Degradation Efficiency (%)
				Before degradation	After degradation	
Amount of catalyst	0.01g	2.30	210		192	78.9
	0.02g	3.07	180	914	178	80.5
	0.03g	4.61	180		157	82.8
	0.04g	1.92	210		241	77.0
Concentration of dye (0.02g catalyst)	$1 \times 10^{-5}\text{M}$	4.22	150	823	153	81.4
	$2 \times 10^{-5}\text{M}$	3.07	180	914	178	80.5
	$3 \times 10^{-5}\text{M}$	-	-	1123	-	-
	$4 \times 10^{-5}\text{M}$	-	-	1256	-	-

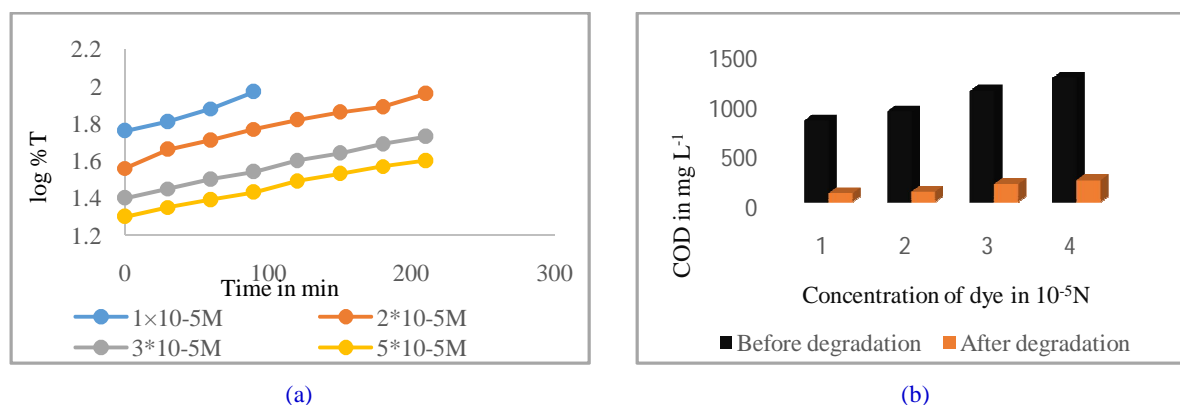


Figure 8. Plot of $\text{Log}\%T$ Vs Time for Different Initial Concentration of Dye (a) and effect of COD upon degradation (b) using Al_2S_3 nanomaterial.

When the visible light strikes the surface of the $\text{Al}_2\text{S}_3/\text{NiS}$ a valance band electron moves into the conduction band thus forming a positively charged hole in the valance band. The conduction band electrons and the valance band holes then migrate to the oxide surface and react with chemisorbed O_2 and/or H_2O molecules to generate reactive oxygen species such as O_2^- , HO_2 , OH radicals, which attack dye molecules and lead to their degradation. On the other hand, the electron in the conduction band can be picked up by the adsorbed dye molecules, leading to the formation of dye radical anion and subsequent reaction of the radical anion can lead to the degradation of dye. In addition, the adsorbed dye molecules may be directly oxidized by the valance band holes to form dye cations which ultimately cause dye degradation. Doping of NiS to Al_2S_3 retards the photo degradation and

hence $\text{Al}_2\text{S}_3/\text{NiS}$ acts as material used for the blackening of sunlight/UV light. The efficiency of photodegradation may be explained by the ability of photocatalyst to trap electrons [26, 27].

Effect of pH: The solution pH is an important variable in the evaluation of aqueous phase mediated photocatalytic reactions. The pH of the solution was adjusted by adding 0.001 M HNO_3 or 0.001 M NaOH solution. The effect of pH was studied at pH 4, pH 6, pH 8 and pH 10 by keeping all other experimental conditions constant. The results are illustrated in figure 9 and tabulated in table 1. The rate of degradation is observed to be slow at pH 6 and high at pH 8. Results of COD effects are illustrated in figure 9. The optimum selected is pH 8 at which photodegradation is high in case of Al_2S_3 catalyst but in case of $\text{Al}_2\text{S}_3/\text{NiS}$ catalyst no photodegradation occurs irrespective of any pH range.

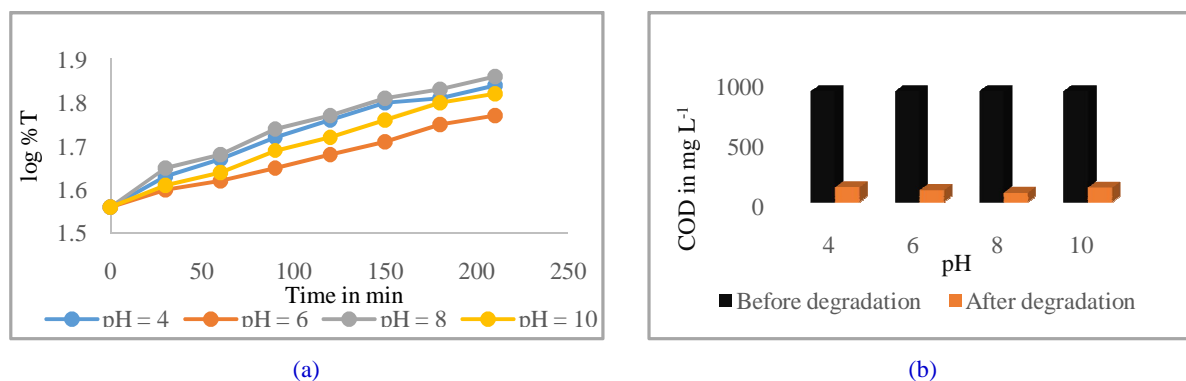


Figure 9. Plot of Log % T Vs Time for different pH of the Dye (a) and effect of COD upon degradation (b) using Al_2S_3 nanoparticle.

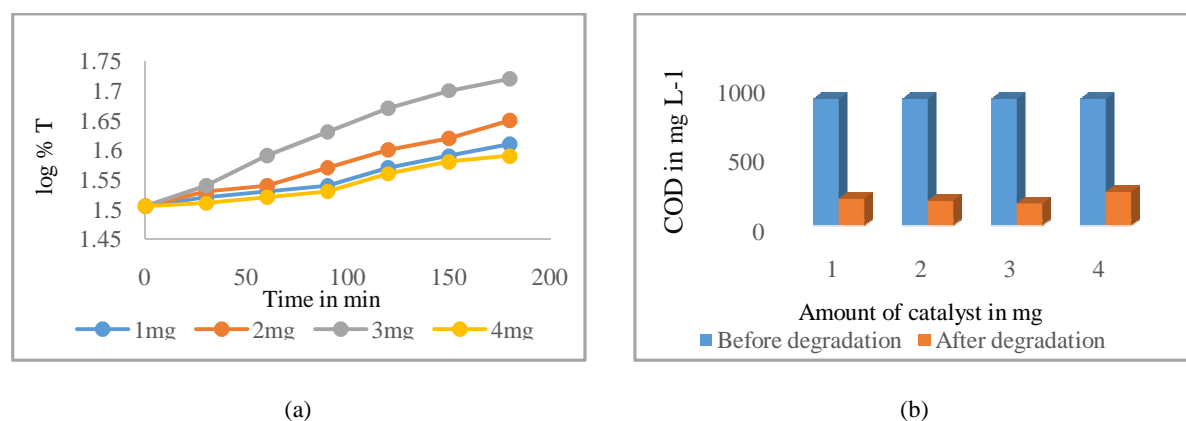


Figure 10. Plot of Log % T Vs Time for Different Amounts of catalyst (a) and Effect of COD upon degradation (b) using $\text{Al}_2\text{S}_3/\text{NiS}$ nanomaterial.

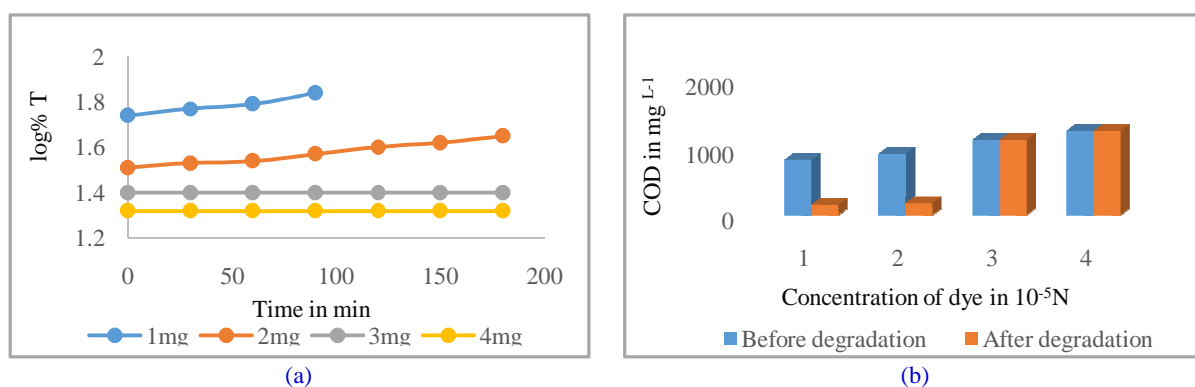


Figure 11. Plot of Log % T Vs Time for Different Amounts of catalyst (a) and Effect of COD upon degradation (b) using $\text{Al}_2\text{S}_3/\text{NiS}$ nanomaterial.

Comparison of photocatalytic efficiency: The band gap of NiS (3.75eV) and Al₂S₃/NiS(2.77eV) is higher than that of Al₂S₃. This supports lower photocatalytic efficiency of Al₂S₃/NiS nanocomposite compared to Al₂S₃ after the formation of Al₂S₃/NiS nanocomposite. Hence, comparison of photocatalytic efficiency of Al₂S₃/NiS nanomaterial with Al₂S₃ and NiS nanomaterials shows the following order (Figure. 12, Table. 3).

Al₂S₃> Al₂S₃/NiS>NiS

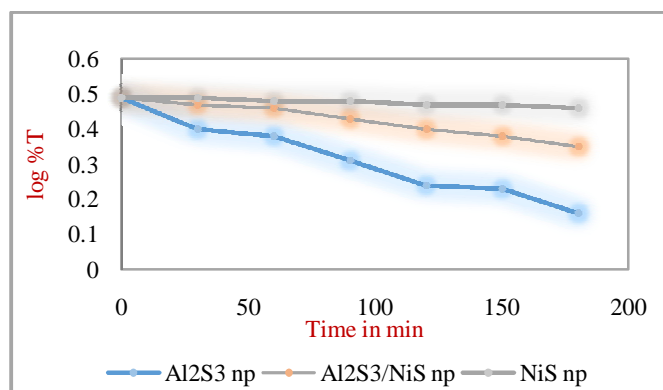


Figure 12. Comparison of photocatalytic efficiency.

Table 3. Rate constant and COD values on using Al₂S₃/NiS, Al₂S₃ and NiS nanomaterials

Nanomaterial (2×10 ⁻⁵ M dye 0.02g catalyst)	Rate constant k s ⁻¹ 10 ⁻⁵	Experimental Time (min)	COD values in mg/ml		Degradation Efficiency (%)
			Before degradation	After Degradation	
Al ₂ S ₃	6.90	180	914	101	88.9
Al ₂ S ₃ /NiS	3.07	180	914	181	80.1
NiS	0.69	180	914	432	47.3

Reuse of the photocatalyst: The possibility of reusing the photocatalyst was examined to see the cost effectiveness of the method. The used photocatalyst was filtered from the first solution and used for fresh MB dye solution. The rate constant at 2×10⁻⁵M of dye concentration is using Al₂S₃ is 6.91 and for reuse of catalyst is 6.52 (Table 1). It was observed that the photocatalytic efficiency was slightly decreased to approximately 80% for the use of second time. Further use of the catalyst showed lesser efficiency.

APPLICATION

The band gap of NiS (3.75eV) and Al₂S₃/NiS (2.77eV) is higher than that of Al₂S₃. This supports lower photocatalytic efficiency of Al₂S₃/NiS nanocomposite compared to Al₂S₃ after the formation of Al₂S₃/NiS nanocomposite. Hence Al₂S₃/NiS nanocomposite can be used as UV light/sunlight blocking material.

CONCLUSION

In the present article Al₂S₃ and Al₂S₃/NiS nanomaterials are synthesized by electrochemical method an eco-friendly method. The photo degradation by this semiconductor offers a green technology, for removal of hazardous components (organic dyes) present in waste water and industrial effluents. Kinetics of photo degradation of Methylene blue suggested that, disappearance of MB follows first order kinetics and nanoparticles can be regenerated, and reused with slightly lesser efficiency. The complete degradation reaction was confirmed, by conducting COD experiment. The doping of NiS to

Al₂S₃ decreases the photocatalytic effect and hence can be used as UV light/sunlight blocking material.

ACKNOWLEDGEMENT

This work has been supported by University of Mysore, Mysuru and the authors acknowledge UGC-BSR and DST-PURSE Program, New Delhi.

REFERENCES

- [1]. H. T. Zhang, G. Wu, X. H. Chen, Synthesis and magnetic properties of NiS_{1+x} nanocrystallines, *Mater. Lett.*, **2005**, 59, 3728-3731.
- [2]. M. Salavati-Niasari, D. Ghanbari, M. R. Loghman-Estarki, Star-shaped PbS nanocrystals prepared by hydrothermal process in the presence of thioglycolic acid Polyhedron, **2012**, 35, 149.
- [3]. M. Salavati-Niasari, A. Badieli, K. Saberyan, Oxovanadium(IV) salophen complex covalently anchored to multi-wall carbon nanotubes (MWNTs) as heterogeneous catalyst for oxidation of cyclooctene, *Chem. Eng. J.*, **2011**, 173, 651-658.
- [4]. E. Esmaeili, M. Salavati-Niasari, F. Mohandes, F. Davar, Modified single-phase hematite nanoparticles via a facile approach for large-scale synthesis, *Chem. Eng. J.*, **2011**, 170, 278.
- [5]. Masoud Salavati-Niasari, Ghazaleh Banaiean-Monfared, Hamid Emadi and Morteza Enhessari. Synthesis and characterization of nickel sulfide nanoparticles via cyclic microwave radiation, *Comptes Rendus Chimie*, **2013**, 16, 929-936.
- [6]. Irem Firtina Ertisand Ismail Boz, Synthesis and Characterization of Metal-Doped (Ni, Co, Ce, Sb) CdS Catalysts and Their Use in Methylene Blue Degradation under Visible Light Irradiation, *Modern Research in Catalysis*, **2017**, 6, 1-14.
- [7]. Abebe Balcha Om Prakash Yadavand Tania Dey, Photocatalytic degradation of methylene blue dye by zinc oxide nanoparticles obtained from precipitation and sol-gel methods, *Environ Sci Pollut Res.*, **2016**, 23, 25485–25493.
- [8]. S. Anandan, A. Vinu, K. L. P. Sheeja Lovely, N. Gokulakrishnan, P. Srinivasu, T. Mori, V. Murugesan, V. Sivamurugan, K. Ariga, Photocatalytic activity of La-doped ZnO for the degradation of monocrotophos in aqueous suspension, *J Mol CatalA Chem.*, **2007**, 266: 149-157.
- [9]. R. J. Wehmschulte, P. P. Power, Low-temperature synthesis of aluminium sulfide in the solvate Al₄S₆(NMe₃)₄ in hydrocarbon solution, *Journal of the American Chemical Society*, **1997**, 119, 9566–9567.
- [10]. R. Oviedo-Roa, J. M. Martinez-Magadan, F. Illas, Correlation between Electronic Properties and Hydrodesulfurization Activity of 4d-Transition-Metal Sulfides, *J. Phys. Chem. B*, **2006**, 110, 7951-66.
- [11]. V. P. Muhamed Shajudheen, V. Senthil Kumar, K. Anitha Rani, A. Uma Maheswari, S. Saravana Kumar, Structural and Optical Properties of NiS Nanoparticles Synthesized by Chemical Precipitation Method, *International Journal of Innovative Research in Science, Engineering and Technology*, **2016**, 5(8), 15099-15103.
- [12]. R. R. AlinRozue, V. Shally, M. Priya Dharshini, Sr. Gerardin Jayam, Structural and Optical properties of Nickel Sulphide(NiS) nanoparticles, *International Journal of NanoScience and Nanotechnology*, **2015**, 6(1), 41-45.
- [13]. X. Jiang, Y. Xie, J. Lu, W. He, L. Zhu, Y. Qian. Preparation and phase transformation of nanocrystalline copper sulfides (Cu₉S₈, Cu₇S₄ and CuS) at low temperature, *J Mater Chem.*, **2000**, 10, 2193–2196.
- [14]. I. P. Parkin, Solid state metathesis reaction for metal borides, silicides, pnictides and chalcogenides: ionic or elemental path ways, *Chem Soc Rev.*, **1996**, 25, 199–207.
- [15]. Zhang YC, Hu XY and Quao, T Shape-controlled synthesis of CuS nanocrystallites via a facile hydrothermal route, *Solid State Commun.*, **2004**, 132, 779-782.

- [16]. Lida Fotouhi and Maral Rezaei, Electrochemical synthesis of copper sulfide nanoparticles, *Microchim Acta*, **2009**, 167, 247–251.
- [17]. Virender Kumar, Kulwinder Singh, Jeewan Sharma, Akshay Kumar, Ankush Vij, and Anup Thakur. Zn doped SnO₂ nanostructures: structural, morphological and spectroscopic properties. *J Mater Sci: Mater Electron* DOI 10.1007/s10854-017-7836-z.
- [18]. K. P. Samskruthi, Sannaiah Ananda, M. B. Nandaprakash, K. S. Chandrakantha. Synthesis and Characterization of SnO₂ and SnO₂/ZnO Nanoparticles by Electrochemical Method: Evaluation of their Performance in Photodegradation of Indigo Carmine Dye and Antibacterial Activity, *Asian Journal of Chemistry*; **2020**, 32(9), 2119-2124.
- [19]. Rakesh, Sannaiah Ananda, Netkal M. Made Gowda, Kithanakere Ramesh Raksha, Synthesis of Niobium Doped ZnO Nanoparticles by Electrochemical Method: Characterization, Photodegradation of Indigo Carmine Dye and Antibacterial Study, *Advances in Nanoparticles*, **2014**, 3, 133-147.
- [20]. L. Wei, C. Shifu, Z. Wei, Z. Sujuan, Titanium Dioxide Mediated Photocatalytic Degradation of Mathamidophos in Aqueous Phase, *Journal of Hazardous Materials*, **2009**, 164, 154-160.
- [21]. M. M. Baig, I. H. Gul, M. Z. Khan, M. T. Mehran, M. S. Akhtar, Binder-free heterostructured MWCNTs/Al₂S₃ decorated on NiCo foam as highly reversible cathode material for high-performance supercapacitors, *Electrochimica Acta*, **2020**, 20(340), 135955.
- [22]. L. Mi, Y. Chen, W. Wei, W. Chen, H. Hou, Z. Zheng. Large-scale urchin-like micro/nano-structured NiS: controlled synthesis, cation exchange and lithium-ion battery applications, *RSC advances*, **2013**, 3(38). 17431-9.
- [23]. K. P. Samskruthi, Sannaiah Ananda, Gubran Alnaggar, Electrochemical synthesis of ZnS/In₂S₃ nanocomposite for photocatalytic oxidation of Acetic acid and its substituents, efficiency compared with ZnS, In₂S₃ and TiO₂, *Chemical Data Collections*, **2021**, 33, 100682.
- [24]. S. Surendran, K.V. Sankar, L. J. Berchmans, R. K. Selvan, Polyol synthesis of α-NiS particles and its physic-chemical properties, *Mater. Sci. Semicond. Process*, **2015**, 33, 16–23.
- [25]. Y. Fazli, S. M. Pourmortazavi, I. Kohsari, M. Sadeghpur, Electrochemical synthesis and structure characterization of nickel sulfide nanoparticles, *Mater. Sci. Semicond. Process*, **2014**, 27, 362–367.
- [26]. M. K Yadav, M. Ghosh, R. Biswas, A. K. Raychaudhuri, A. Mookerjee,. Band gap variation in Mg- and Cd-doped ZnO nanostructures and molecular clusters, *Physical Review B*, **2007**, 76, DOI. 195450.
- [27]. G. Chaitanya Lakshmi, S. Ananda, R. Somashekar, C. Ranganathaiah. Synthesis of ZnO/ZrO₂ Nanocomposites by Electrochemical Method and Photocatalytic Degradation of Fast Green Dye, Paper Dyeing and Printing Press Effluent. *International Journal of Advanced Materials Science*, **2012**, 3(3), 221-237.
- [28]. Hosaholalu Balakrishna Uma, Sannaiah Ananda, Vittal Ravishankar Rai, Synthesis and Characterization of In₂S₃ nanoparticles by Electrochemical method: Evaluation of its performance in photo-assisted degradation of indigo carmine dye, antibacterial and antimutagenic activity studies, *International Journal of Nanotechnology and Application*, **2017**, 7(3), 1-16.
- [29]. Yousef Fazli, Seied Mahdi Pourmortazavi, Iraj Kohsari, Meisam Sadeghpour Karimi, Majid Tajdari. Synthesis, characterization and photocatalytic property of nickel sulfide nanoparticles, *J Mater Sci: Mater Electron*, **2016**, 27, 7192–7199.
- [30]. M. Banerjee, L. Chongad, A. Sharma, Structural and Optical Properties of Pure and Copper Doped NiS Nanoparticles, *Research Journal of Recent Sciences*, **2013**, 2, 326-329.
- [31]. H. C. Charan Kumar, R. Shilpa, Sannaiah Ananda, Synthesis and Characterization of Al-Doped ZnO Nanoparticles by Electrochemical Method: Photodegradation Kinetics of Methylene Blue Dye and Study of Antibacterial Activities of Al-Doped ZnO Nanoparticles, *J. Applicable Chem*, **2020**, 9(1), 9-21.
- [32]. H. C Charan Kumar, R. Shilpa, V. Ravi Shankar Rai, Sannaiah Ananda. Synthesis and Characterization of NiO Nanoparticles by Electrochemical Method: Photodegradation Kinetics of Indigo Carmine Dye and Study of Antibacterial Activities of NiO Nanoparticles, *J. Applicable Chem.*, **2019**, 8(2), 622-633.

- [33]. K. R. Raksha, S. Ananda, An investigation on: kinetics of photo catalysis, electrical property and biological activity of electrochemically synthesized ZnS and Ru: ZnS nano photocatalysis. *J. Applicable Chem.*, 2014, 3, 397-412.